IEEE Photonics Journal
An IEEE Photonics Society Publication

Open Access

Flexible Frequency-Hopping Microwave Generation by Dynamic Control of Optically Injected Semiconductor Laser

Volume 8, Number 6, December 2016

Pei Zhou, *Student Member, IEEE*
Fangzheng Zhang, *Member, IEEE*
Xingwei Ye, *Student Member, IEEE*
Qingshui Guo
Shilong Pan, *Senior Member, IEEE*

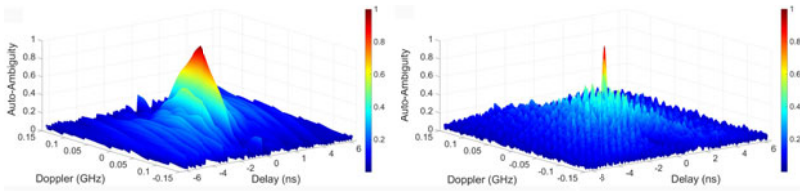

DOI: 10.1109/JPHOT.2016.2629082
1943-0655 © 2016 IEEE

Flexible Frequency-Hopping Microwave Generation by Dynamic Control of Optically Injected Semiconductor Laser

Pei Zhou, *Student Member, IEEE*, Fangzheng Zhang, *Member, IEEE*, Xingwei Ye, *Student Member, IEEE*, Qingshui Guo, and Shilong Pan, *Senior Member, IEEE*

Key Laboratory of Radar Imaging and Microwave Photonics, Ministry of Education, Nanjing University of Aeronautics and Astronautics, Nanjing 210016, China

DOI:10.1109/JPHOT.2016.2629082

Manuscript received August 29, 2016; revised November 8, 2016; accepted November 12, 2016. Date of publication November 16, 2016; date of current version December 7, 2016. This work was supported in part by the National Science Foundation of China (NSFC) Program under Grant 61401201, Grant 61422108, and Grant 61527820; in part by the NSFC Program of Jiangsu Province under Grant BK20140822; in part by the Aviation Science Foundation of China under Grant 2015ZC52024; in part by the Postdoctoral Science Foundation of China under Grant 2015T80549 and Grant 2014M550290; and in part by the Fundamental Research Funds for the Central Universities. Corresponding authors: F. Zhang and S. Pan (e-mail: zhangfangzheng@nuaa.edu.cn; pans@ieee.org).

Abstract: Under proper optical injection, period-one (P1) dynamics of an optically injected semiconductor laser can be excited by undamping the relaxation resonance of the semiconductor through Hopf bifurcation. The output intensity would oscillate at a microwave frequency, i.e., the P1 frequency. After optical-to-electrical conversion, a microwave signal can be generated with its frequency determined by the detuning frequency and the injection strength. Therefore, it provides a convenient way to dynamically control the instantaneous frequency of the generated microwave signal by manipulating the injection strength. In this work, a flexible frequency-hopping (FH) microwave waveform generator by dynamic control of an optically injected semiconductor laser is proposed and demonstrated. The system has a compact structure, and the key device is a commercial semiconductor laser. The generated FH microwave waveform has a high degree of flexibility, i.e., the central frequency, bandwidth, sequence length, and frequency order can be easily adjusted. A proof-of-concept experiment is carried out. Wideband (>10 GHz) stepped linear and Costas sequence are successfully generated. Autoambiguity functions of the generated frequency-hopping sequences are also investigated. The experimental results can verify the feasibility of the proposed FH waveform generator, which may find wide applications in future radar and communications systems.

Index Terms: Microwave generation, frequency-hopping, semiconductor lasers, optical injection, microwave photonics.

1. Introduction

Semiconductor lasers are inherently nonlinear devices. When a semiconductor laser is subject to an incoming optical carrier, rich nonlinear dynamics can be excited, such as stable injection locking, periodic oscillations, and chaos [1]–[4]. The resultant dynamical characteristics can be well

controlled by the external operational parameters, including the detuning frequency and injection strength. Due to its unique temporal and spectral characteristics, nonlinear dynamics of an optically injected semiconductor laser have been utilized for many interesting and novel applications. For example, stable injection locking dynamics has been demonstrated for modulation bandwidth enhancement, chirp and noise reduction [5]–[7]. Chaotic dynamics has been studied for cryptography, high-speed random number generation, high-resolution ranging and imaging [8]–[11]. Period-one (P1) dynamics has been investigated for photonic microwave amplification, single-sideband (SSB) modulation, and optical frequency conversion [12]–[15]. Besides, P1 dynamics has been applied for photonic microwave generation with a frequency range up to 100 GHz [16]–[18]. In this study, we propose to use controlled P1 dynamics of an optically injected semiconductor laser for generating flexible frequency-hopping (FH) microwave waveforms.

Frequency-hopping microwave waveforms are widely used in applications such as radar, communication and electronic warfare systems [20], [21]. In communication systems, FH technique can be used to enhance the network capacity and the anti-interference ability. In radar systems, the large time-bandwidth product (TBWP) of FH waveforms can bring advantages of increased detection range and improved range resolution. In addition, compared to the poor two-dimension united resolution of range and velocity of linear frequency-modulated (LFM) signal caused by the large range-Doppler coupling, specially coded FH microwave waveform, e. g., wideband Costas sequence, which has a thumbtack-shaped auto-ambiguity function, has been researched for simultaneously achieving high resolutions for both range and velocity detections. However, due to the limited speed and bandwidth of current electronic circuits, FH microwave waveforms generated by pure electrical technologies have a low central frequency and small bandwidth. Thanks to the inherent advantages of high frequency and large bandwidth, several photonic approaches have been proposed for generating FH microwave waveforms [22]–[26]. For instance, a frequency-swept microwave signal is generated by beating a wavelength sweeping distributed feedback (DFB) laser with an optical carrier having a fixed wavelength [22] or another wavelength sweeping optical signal [23]. This method can be adapted to generate wideband FH microwave waveforms, but suffers from a poor quality of generated FH microwave waveform because of the serious dynamic linewidth broadening of the laser beam during wavelength sweeping. Besides, the noncoherent phase relation between the two lasers would further degrade the signal quality after optical-to-electrical conversion. In [24], Li *et al*. demonstrated a FH microwave waveform generation scheme based on a frequency-tunable optoelectronic oscillator (OEO) incorporating a polarization-maintaining phase-shifted fiber Bragg grating (PM-PSFBG). In the system, the PM-PSFBG has a polarization-dependent response. Thus, the output frequency can be changed by controlling the polarization state. The drawback is that the number of frequency points is limited, and the frequency is hard to be tuned. FH microwave waveforms can also be generated using a photonic arbitrary waveform generator based on optical pulse shaping and frequency-to-time mapping [25], [26], but the use of femtosecond pulsed laser and optical pulse shaper significantly increases the complexity and cost of the whole system.

In this paper, we propose and experimentally demonstrate the generation of FH microwave waveform based on an optically injected semiconductor laser. Under proper optical injection, P1 dynamics of a semiconductor laser can be excited by undamping the relaxation resonance of the semiconductor through Hopf bifurcation. The output intensity oscillates at a microwave frequency. After optical-to-electrical conversion, a frequency tunable microwave signal can be generated with its frequency determined by the detuning frequency and injection strength. Therefore, by properly controlling the injection strength, wideband FH microwave waveform can be achieved. The generated FH microwave waveform has a high degree of flexibility, and its center frequency, bandwidth, sequence length, as well as the frequency order can be easily adjusted. A proof-of-concept experiment is carried out. In the experiment, wideband ($>$10 GHz) stepped linear and Costas sequence of length 10 are successfully generated. Auto-ambiguity functions of the generated frequency-hopping sequences are also investigated. The feasibility of adjusting the different parameters of the generated FH microwave waveforms is also verified.

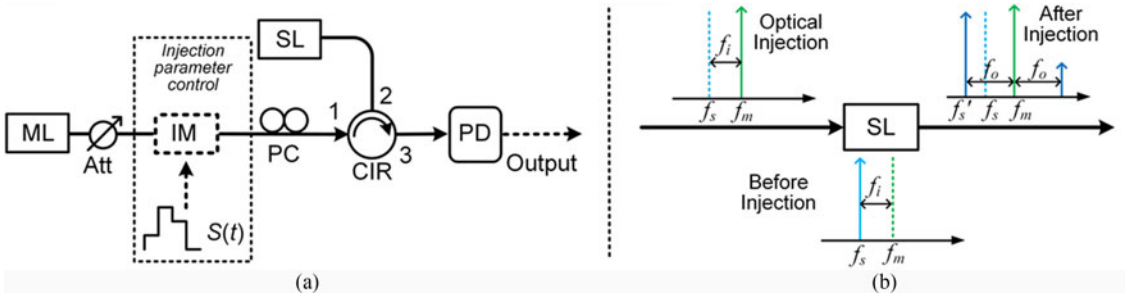

Fig. 1. (a) Schematic configuration of the proposed photonic FH microwave waveform generator. (b) Operation principle of P1 dynamics in optically injected semiconductor laser. ML: master laser, Att: optical attenuator; IM: intensity modulator, $S(t)$: control signal; PC: polarization controller, CIR: optical circulator; SL: slave laser, PD: photo-detector.

2. Principle

The schematic configuration of the proposed FH microwave waveform generator is shown in Fig. 1(a). The slave laser (SL) is a semiconductor laser with a free-running frequency f_s. A continuous wave (CW) light from a master laser (ML) with frequency f_m is injected to the slave laser through an optical circulator. The injection light pulls the intracavity field oscillation of the slave laser toward f_m by locking the optical phase of the laser, leading to the frequency component at f_m at the output of the slave laser. Meanwhile, the necessary gain for the slave laser is modified through optical injection. According to the antiguidance effect, the refractive index inside the cavity changes, resulting in the red shift of the cavity resonance from f_s to f_s'. Such an injection-shifted cavity resonance competes dynamically with the injection-imposed laser oscillation, which radically modifies the dynamics of the injected laser. Under proper injection conditions, this would lead to the emergence of asymmetric double-sideband spectrum through Hopf bifurcation. As shown in Fig. 1(b), such a spectral characteristic is a typical signature of P1 dynamics in optically injected semiconductor lasers [2], [12]–[18]. When the output signal from the slave laser is sent to a PD, a microwave signal having frequency f_o ($f_o = f_m - f_s'$) can be generated. Since the cavity resonance shift depends on the gain reduction which is determined by the injection strength and the detuning frequency between the master and slave lasers, the beating microwave frequency after photo-detector (PD) is considerably dependent on the injection condition. Here, the injection strength is characterized by the injection parameter ξ, which is defined as the square root of the power ratio between the injected light and the free-running slave laser, i.e., the injection parameter ξ is proportional to the optical amplitude of the light injected to the slave laser. For a fixed master-slave detuning frequency f_i ($f_i = f_m - f_s$), the microwave frequency f_o would increase approximately linearly with the injection parameter over a large range [18], [19]. In the system, a control signal $S(t)$ is applied to an intensity modulator (IM) to manipulate the amplitude of the injection light before it is sent to the slave laser. By setting the control signal $S(t)$ to be a two-level square wave, a microwave waveform with its frequency hopping between two frequencies will be generated. If $S(t)$ is a multi-level signal, a FH microwave waveform with multiple frequencies, i.e., frequency-hopping sequence, can be obtained. During this process, the FH range can be enlarged by choosing a large amplitude variation of the injection light, and the specific frequencies can be tuned by changing the initial injection parameter. In addition, the sequence length and the frequency order of the FH sequences can also be adjusted by simply changing the control signal. As a result, the proposed FH microwave waveform generator has a high degree of flexibility and major parameters of the generated FH microwave waveform can be changed by adjusting the applied electrical control signal $S(t)$.

3. Experimental Demonstration

A proof-of-concept experiment is carried out based on the setup in Fig. 1(a). The experimental setup is given in Fig. 2. A laser source (Agilent N7714A) with a wavelength of 1552.870 nm and a

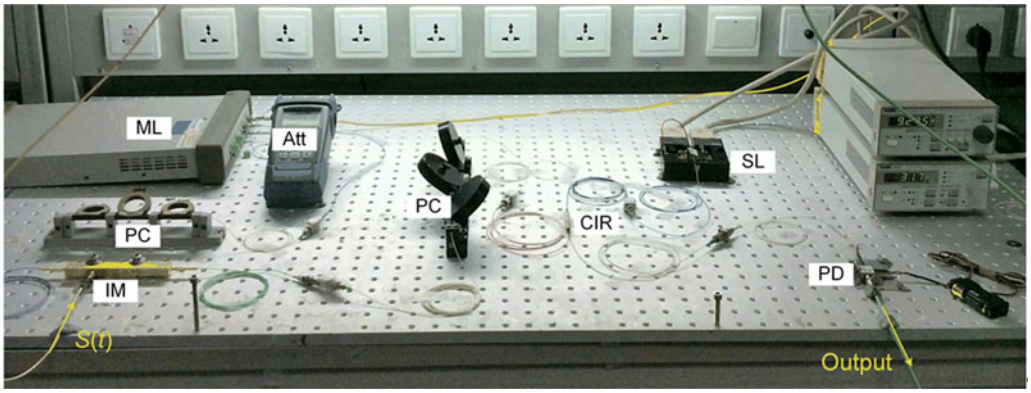

Fig. 2. Experimental setup.

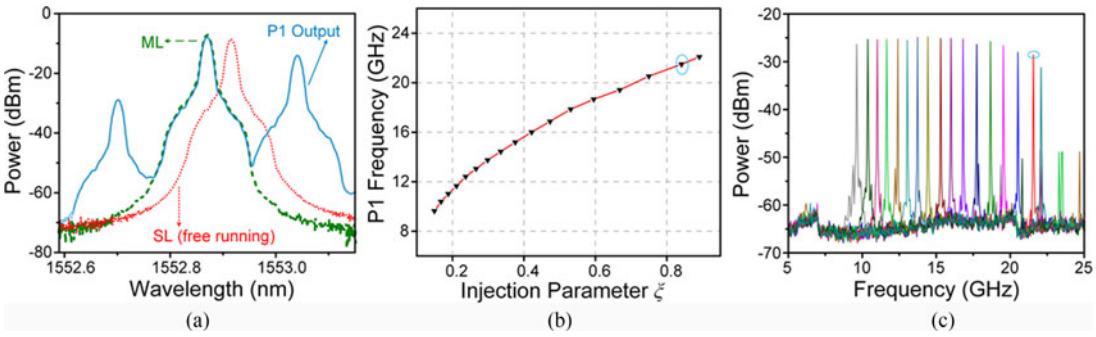

Fig. 3. (a) Optical spectra of the injection light (green dashed curve), free-running slave laser (red dot curve), and the injected slave laser when $\xi = 0.84$ (blue solid curve). (b) Measured output frequency as a function of the injection parameter. (c) Corresponding electrical spectra.

power of 13.5 dBm is applied as the master laser. Thereafter, a variable optical attenuator is used to adjust the power of the injection light. The CW light from the master laser is sent to an "injection parameter control" unit which consists of a 10 Gb/s Mach-Zehnder modulator (MZM, Lucent 2623NA) and an electrical control signal generated by a 120-MHz arbitrary waveform generator (Agilent 81150A). The slave laser (Actech LD15DM) is a DFB laser biased at 31.7 mA, about 5 times of the threshold. The free-running wavelength and power of the slave laser is 1552.915 nm and 4.98 dBm, respectively. Throughout the experiments, the master-slave detuning frequency is fixed at 5.6 GHz, unless otherwise specified. Before the optical circulator, a polarization controller (PC) is used to align the polarization of the injection light with that of the slave laser to maximize the injection efficiency. At the output of the optical circulator (port 3), a PD (u2t XPDV2120RA) with 40 GHz bandwidth is used to implement optical-to-electrical conversion. The generated FH microwave waveform is observed by an 80 GSa/s real-time oscilloscope (Keysight DSO-X 92504A). The optical spectrum is measured by an optical spectrum analyzer (Yokogawa AQ6370C).

First, the electrical control signal is not applied, and the power of the CW light injected to the slave laser is adjusted by the optical attenuator. The master-slave detuning frequency is 5.6 GHz. Fig. 3(a) shows the optical spectrum of P1 dynamics when ξ equals to 0.84 (blue solid curve). For comparison, the spectra of the injection light (green dashed curve) and the free-running slave laser (red dot curve) are also shown. As can be seen, two highly dominant wavelength components separated by the P1 oscillation frequency $f_o = 21.5$ GHz is observed after optical injection. The oscillation frequency (f_o) as a function of the injection parameters ξ is also measured by a 40-GHz electrical spectral analyzer (R&S FSV40). In this process, the injection parameter is changed by tuning the optical power injected to the slave laser, and it is calculated according to the injection power measured at the output port of the circulator connected to the slave laser (port 2) and

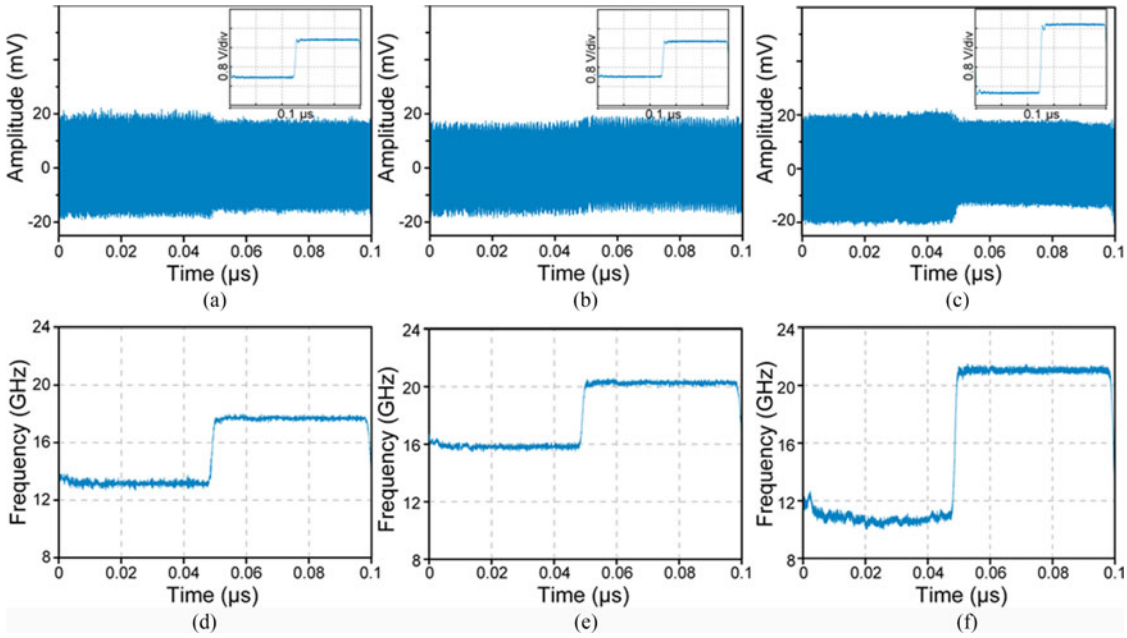

Fig. 4. (a)–(c) Measured temporal waveforms under different injection conditions. (Insets) Corresponding control signal $S(t)$). (d)–(f) Recovered instantaneous frequency corresponding to (a)–(c), respectively.

the optical power of the free running slave laser. As shown in Fig. 3(b), the oscillation frequency (f_o) increases almost linearly with the injection parameter ξ over a large frequency range, except the slightly nonlinear range at lower injection parameters [19]. Fig. 3(c) shows the corresponding electrical spectra of the generated microwave signal after optical-to-electrical conversion. It should be noted that the generated microwave using optically injected semiconductor laser has a relatively large 3-dB linewidth on the order of megahertz, which is mainly caused by the spontaneous emission noise of the injected laser. This problem can be possibly solved by using an optoelectronic feedback structure reported in [16], [17]. What's more, the P1 output spectrum in Fig. 3(a) (blue solid curve) corresponds to the circled circumstances in Fig. 3(b) and (c).

Then, a 10 MHz two-level square wave is applied to the MZM, which is biased at the quadrature point. At the output of the PD, a FH microwave waveform with a temporal period of 0.1 μs is measured. By simply changing the initial injection parameter and the amplitude of the control signal $S(t)$, the specific frequencies and the bandwidth of generated FH microwave waveforms can be tuned. Fig. 4(a)–(c) are the measured temporal waveforms under different injection conditions and the insets are the waveforms of corresponding control signal $S(t)$. Fig. 4(d)–(f) show the recovered instantaneous frequency of the microwave waveform based on Hilbert transformation corresponding to the circumstance in Fig. 4(a)–(c), respectively. At first, the initial injection parameter is set to $\sim$0.6, and the amplitude of $S(t)$ is $\sim$1.6 V. The generated FH waveform is shown in Fig. 4(a). As can be seen in Fig. 4(d), the instantaneous frequency is bouncing between 13.1 and 17.6 GHz, indicating a FH bandwidth of 4.5 GHz. Then, as shown in Fig. 4(b) and (e), by changing the initial injection parameter from $\sim$0.6 to $\sim$0.84 using the optical attenuator, the instantaneous frequency of generated FH microwave waveform is hopping from 15.8 to 20.3 GHz, and the FH bandwidth remains 4.5 GHz. Besides, when the amplitude of $S(t)$ is increased to $\sim$2.6 V, the variation of optical injection parameter is enlarged, and hence, an FH waveform with a larger FH bandwidth is achieved. As shown in Fig. 4(c) and (f), the instantaneous frequency changes between 10.5 and 21.0 GHz, indicating a FH range as large as 10.5 GHz. The tuning time of control signal (τ_1) and corresponding instantaneous frequency (τ_2) are also investigated. Thanks to the fast dynamical rate parameters, typically in the range of 10^9–10^{11} s^{-1}, the dynamical behavior of a typical semiconductor varies at a sub-nanosecond time scale [3]. In the experiment, (τ_1, τ_2) is measured to be about (1.5 ns,

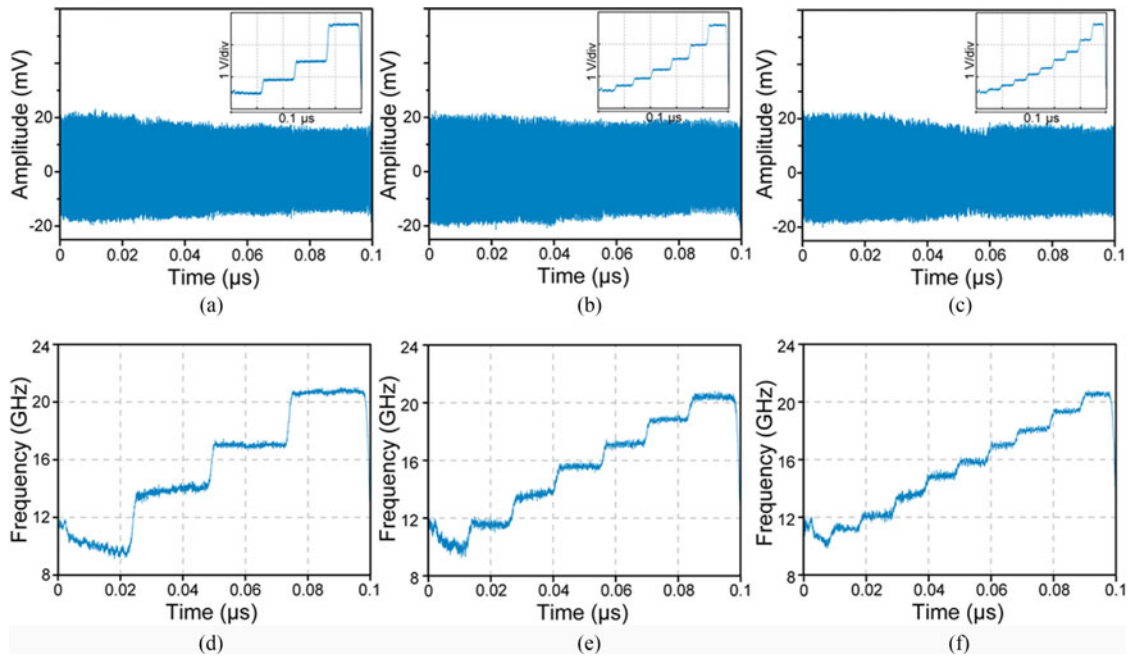

Fig. 5. (a)–(c) Measured temporal waveforms under different injection conditions. (Insets) Corresponding control signal $S(t)$. (d)–(f) Recovered instantaneous frequency corresponding to (a)–(c), respectively.

1.6 ns), (1.5 ns, 1.5 ns) and (1.5 ns, 1.6 ns) for Fig. 4(a)–(c), respectively. It shows that tuning time of instantaneous frequency is consistent with that of corresponding control signal.

If a multi-level (>2) control signal $S(t)$ is applied to the MZM to control the injection parameter, a FH microwave waveform with multiple frequencies, i.e., frequency-hopping sequence, can be obtained. By simply increasing the levels of the electrical control signal $S(t)$, the sequence length of generated FH sequences can be increased. Fig. 5(a)–(c) are the measured temporal waveforms of stepped linear sequence with different sequence length and the insets are the waveforms of corresponding control signal $S(t)$. Here, the control signals has unevenly spaced levels to compensate for the nonlinearity in the $f_o - \xi$ function. The average power of the generated FH waveforms is around –35 dBm. Fig. 5(d)–(f) show the recovered instantaneous frequency of the microwave waveform corresponding the circumstance in Fig. 5(a)–(c), respectively. Fig. 5(a) and (d) shows the results when a 4-level control signal is adopted. As can be seen, a stepped linear sequence with a length $N = 4$ is generated with a temporal period of 0.1 μs. The four frequencies are 10.3, 13.8, 17.3, and 20.8 GHz. Similarly, by properly adapting the control signal, stepped linear sequence with a length $N = 7$ and 10 are also generated, which are separately plotted in Fig. 5(b) and (c). From the instantaneous frequency curves in Fig. 5(e) and (f), seven and ten linearly increased frequencies are observed, respectively.

In addition, the frequency order of the FH sequences can also be adjusted by simply setting the control signal. One example is the generation of microwave Costas sequence, which has been widely used in applications like radar engineering, synchronization, and communications. Compared to the poor two-dimension resolution of range and velocity by using linear frequency-modulated signal and stepped linear sequence, microwave Costas sequence is proven to have an optimal (thumbtack) auto-ambiguity function and higher range-Doppler resolution. Here, we specifically implement Costas sequences with a length N = 4, 7, and 10, which are described in Table I. In order to realize these sequences, the control signals applied to MZM are set to have a similar pattern to Costas array. Fig. 6(a)–(c) show the generated Costas sequences with different length and a temporal period of 0.1 μs, and the average power is around –35 dBm. The insets are the waveforms of corresponding control signal $S(t)$. Their instantaneous frequency versus time are separately plotted in Fig. 6(d)–(f). As can be seen, the transitions are close to what we expected: 4,

TABLE I
Costas Sequences

Length	Frequency hopping sequence ordering
4	2, 4, 3, 1
7	4, 7, 1, 6, 5, 2, 3
10	2, 4, 8, 5, 10, 9, 7, 3, 6, 1

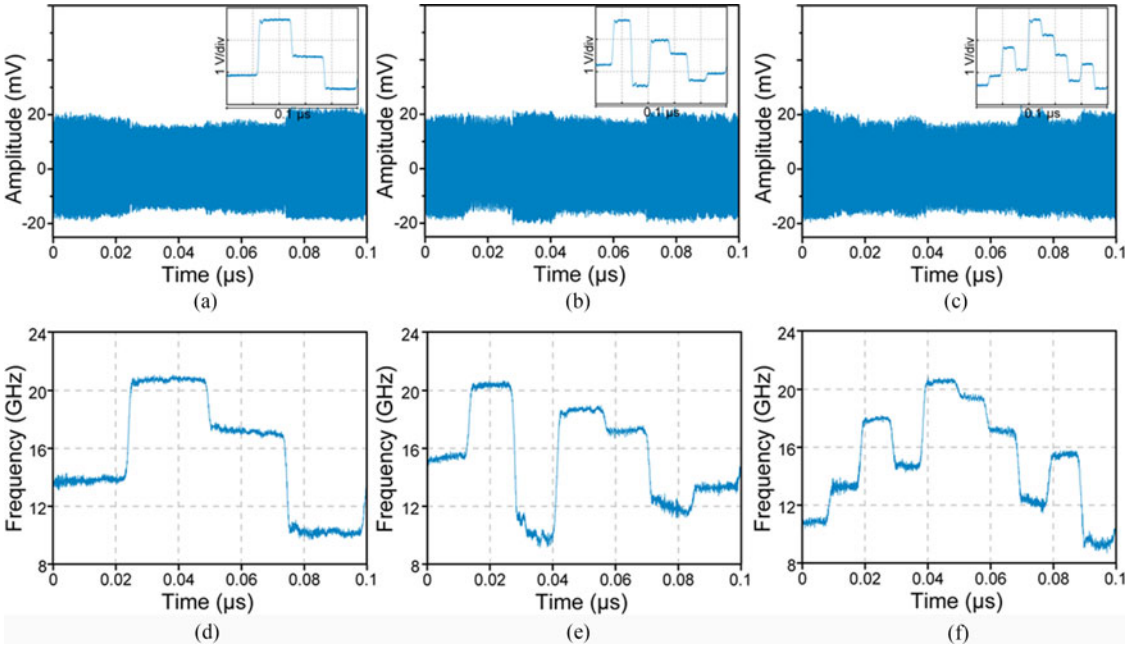

Fig. 6. (a)–(c) Measured temporal waveforms under different injection conditions (Insets) Corresponding control signal $S(t)$). (d)–(f) Recovered instantaneous frequency corresponding to (a)–(c), respectively.

7 and 10 frequencies are evenly spaced between ∼10 and ∼20.5 GHz and their frequency order are in agreement with the ordering in Table I.

A criterion often used for evaluating the range-Doppler resolution is the auto-ambiguity function [19]. This function measures the compression of a microwave waveform both in time domain (corresponding to range) and frequency domain (corresponding to Doppler). To further show the performance characteristic of the generated FH sequences, the auto-ambiguity functions are calculated offline. Fig. 7 shows the comparison of auto-ambiguity functions of (a) stepped linear and (b) Costas sequence when $N = 10$. As can be seen in Fig. 7(a), if the frequencies are monotonically increasing, which can be viewed as a stepped approximation of an LFM signal, a ridge in its auto-ambiguity function can be observed, leading to a large range-Doppler coupling with a reduced range-Doppler resolution. In comparison, when the order of frequencies meets the Costas sequence, a thumbtack-like auto-ambiguity function is obtained, as shown in Fig. 7(b), which indicates that the range-Doppler coupling is reduced and the range-Doppler resolution is improved [20]. The main lobe of the auto-ambiguity function has a full-width half-maximum (FWHM) of ∼94 ps in delay and ∼ 11.2 MHz in Doppler, respectively.

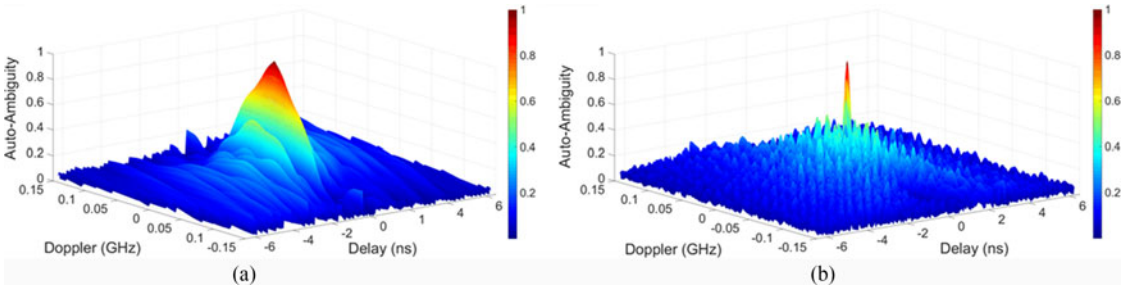

Fig. 7. Comparison of auto-ambiguity functions for N = 10 (a) stepped linear and (b) Costas sequence.

4. Conclusion

We have proposed a flexible photonic FH microwave waveform generator using controlled dynamics of an optically injected semiconductor laser. The proposed system mainly consists of a commercial semiconductor laser as slave laser and an amplitude controlled master laser, leading to a low-cost and simple structure. Besides, the proposed FH microwave waveform generator has a high degree of flexibility and major parameters of the generated FH microwave waveform can be changed by adjusting the applied electrical control signal $S(t)$. A proof-of-concept experiment is carried out. In the experiment, wideband ($>$10 GHz) stepped linear and Costas sequence with different length are successfully generated. Auto-ambiguity functions of the generated frequency-hopping sequences are also investigated. In addition, the feasibility of adjusting the center frequency, bandwidth, and sequence length of the generated FH microwave waveforms is also verified. The experimental results can confirm the good performance of the proposed technique, which may find wide applications in future radar and other microwave systems.

References

[1] V. Annovazzi Lodi, S. Donati, and M. Manna, "Chaos and locking in a semiconductor laser due to external injection," *IEEE J. Quantum Electron.*, vol. 30, no. 7, pp. 1537–1541, Jul. 1994.
[2] T. B. Simpson, J. M. Liu, K. F. Huang, and K. Tai, "Nonlinear dynamics induced by external optical injection in semiconductor lasers," *Quantum Semiclassical Opt.*, vol. 9, no. 5, pp. 765–784, May 1997.
[3] S. Wieczorek, B. Krauskopf, T. B. Simpson, and D. Lenstra, "The dynamical complexity of optically injected semiconductor lasers," *Phys. Rep.*, vol. 416, nos. 1/2, pp. 1–128, Sep. 2005.
[4] S. K. Hwang and J. M. Liu, "Dynamical characteristics of an optically injected semiconductor laser," *Opt. Commun.*, vol. 183, nos. 1–4, pp. 195–205, Sep. 2000.
[5] T. B. Simpson, J. M. Liu, and A. Gavrielides, "Bandwidth enhancement and broadband noise reduction in injection-locked semiconductor lasers," *IEEE Photon. Technol. Lett.*, vol. 7, no. 7, pp. 709–711, Jul. 1995.
[6] J. M. Liu, H. F. Chen, X. J. Meng, and T. B. Simpson, "Modulation bandwidth, noise, and stability of a semiconductor laser subject to strong injection locking," *IEEE Photon. Technol. Lett.*, vol. 9, no. 10, pp. 1325–1327, Oct. 1997.
[7] T. B. Simpson, J. M. Liu, and A. Gavrielides, "Bandwidth enhancement and broadband noise reduction in injection-locked semiconductor lasers," *IEEE Photon. Technol. Lett.*, vol. 7, no. 7, pp. 709–711, Jul. 1995.
[8] V. Annovazzi-Lodi, S. Donati, and A. Scire, "Synchronization of chaotic injected-laser systems and its application to optical cryptography," *IEEE J. Quantum Electron.*, vol. 32, no. 6, pp. 953–959, Jun. 1996.
[9] A. Argyris *et al.*, "Chaos-based communications at high bit rates using commercial fibre-optic links," *Nature*, vol. 438, pp. 343–346, Nov. 2005.
[10] A. Uchida *et al.*, "Fast physical random bit generation with chaotic semiconductor lasers," *Nature Photon.*, vol. 2, pp. 728–732, Nov. 2008.
[11] F. Y. Lin and J. M. Liu, "Chaotic lidar," *IEEE J. Sel. Topics Quantum Electron.*, vol. 10, no. 5, pp. 991–997, Sep./Oct. 2004.
[12] Y. H. Hung and S. K. Hwang, "Photonic microwave amplification for radio-over-fiber links using period-one nonlinear dynamics of semiconductor lasers," *Opt. Lett.*, vol. 38, no. 17, pp. 3355–3358, Sep. 2013.
[13] Y. H. Hung, C. H. Chu, and S. K. Hwang, "Optical double-sideband modulation to single-sideband modulation conversion using period-one nonlinear dynamics of semiconductor lasers for radio-over-fiber links," *Opt. Lett.*, vol. 38, no. 9, pp. 1482–1484, May 2013.
[14] S. K. Hwang, H. F. Chen, and C. Y. Lin, "All-optical frequency conversion using nonlinear dynamics of semiconductor lasers," *Opt. Lett.*, vol. 34, no. 6, pp. 812–814, Mar. 2009.
[15] S. K. Hwang, J. M. Liu, and J. K. White, "Characteristics of period-one oscillations in semiconductor lasers subject to optical injection," *IEEE J. Sel. Topics Quantum Electron.*, vol. 10, no. 5, pp. 974–981, Sep. 2004.

[16] S. C. Chan and J. M. Liu, "Tunable narrow-linewidth photonic microwave generation using semiconductor laser dynamics," *IEEE J. Sel. Top. Quantum Electron.*, vol. 10, no. 5, pp. 1025–1032, Sep. 2004.
[17] P. Zhou, F. Z. Zhang, B. D. Gao, and S. L. Pan, "Optical pulse generation by an optoelectronic oscillator with optically injected semiconductor laser," *IEEE Photon. Technol. Lett.*, vol. 28, no. 17, pp. 1827–1830, Sep. 2016.
[18] S. C. Chan, S. K. Hwang, and J. M. Liu, "Radio-over-fiber AM-to-FM upconversion using an optically injected semiconductor laser," *Opt. Lett.*, vol. 31, no. 15, pp. 2254–2256, Aug. 2006.
[19] F. Mogensen, H. Olesen, and G. Jacobsen, "Locking conditions and stability properties for a semiconductor laser with external light injection," *IEEE J. Quantum Electron.*, vol. QE-21, no. 7, pp. 784–793, Jul. 1985.
[20] M. Skolnik, *Radar Handbook*, 3rd ed. New York, NY, USA: McGraw-Hill, 2008.
[21] M. K. Simon, *Spread Spectrum Communications Handbook*. New York, NY, USA: McGraw-Hill, 1994.
[22] J. M. Wun, C. C. Wei, J. Chen, C. S. Goh, S. Y. Set, and J. W. Shi, "Photonic chirped radio-frequency generator with ultra-fast sweeping rate and ultra-wide sweeping range," *Opt. Exp.*, vol. 21, no. 3, pp. 11475–11481, May 2013.
[23] O. L. Coutinho, J. Zhang, and J. Yao, "Photonic generation of a linearly chirped microwave waveform with a large time-bandwidth product based on self-heterodyne technique," in *Proc. Int. Topical Meeting Microw. Photon.*, Paphos, Cyprus, 2015, pp. 1–4.
[24] W. Li, W. Zhang, and J. Yao, "Frequency-hopping microwave waveform generation based on a frequency-tunable optoelectronic oscillator," in *Proc. Opt. Fiber Commun. Conf. Exhib.*, San Francisco, CA, USA, 2014, pp. 1–3.
[25] C. Wang and J. P. Yao, "Large time-bandwidth product microwave arbitrary waveform generation using a spatially discrete chirped fiber Bragg grating," *J. Lightw. Technol.*, vol. 28, no. 11, pp. 1652–1660, Jun. 2010.
[26] A. Rashidinejad and A. M. Weiner, "Photonic radio-frequency arbitrary waveform generation with maximal time-bandwidth product capability," *J. Lightw. Technol.*, vol. 32, no. 20, pp. 3383–3393, Oct. 2014.